INTERNATIONAL JOURNAL OF INTEGRATED ENGINEERING
ISSN: 2229-838X e-ISSN: 2600-7916

IJIE

Vol. 16 No. 5 (2024) 250-264
https://publisher.uthm.edu.my/ojs/index.php/ijie

A Novel PWM Inverter Topology for Intuitive Motion Controls of EV With BLDC Motor

Ranjan Pramanik[1] , Jatin K. Pradhan[2]* , B.B.Pati[1]

[1] *Department of Electrical Engineering, VSSUT Burla, Sambalpur, 768017, INDIA*
[2] *Department of Electrical Engineering, NIT Rourkela, Rourkela, 769008, INDIA*

*Corresponding Author: er.jatinpradhan@gmail.com
DOI: https://doi.org/10.30880/ijie.2024.16.05.019

Article Info

Received: 16 November 2023
Accepted: 21 June 2024
Available online: 12 August 2024

Keywords

Inverter switching, BLDC motor, Pole placement, PID control

Abstract

Permanent magnet brushless DC (PMBLDC) motors are having a huge impact on next-generation electric vehicle (EV) applications due to their high-performance accuracy and reliability in the motion control area. This paper offers a unique inverter switching method to control the PMBLDC motor for high voltage (HV) e-mobility applications. In this work, the speed of a permanent BLDC motor is controlled by a suitable inverter switching selections via inverter mapped with motor position. Hence, the anticipated switching method is depended on identifying the sector position and selecting the suitable control logic for switching inverter. Here, a feedback and feedforward loop design based control logic are used for tracking and improved input-output performance, respectively. The feedback loop used a proportional-integral-derivative (PID) controller. The gains of the PID controller are tuned by using dominant pole placement technique to ensure robust loop performance. Further, a feed forward gain is designed to improve the input output performance. Simulations are carried out with a developed hardware set-up of BLDC motor with AKD interface device to validate the system performances experimentally.

1. Introduction

New generation electric vehicle (EV) or hybrid electric vehicle (HEV) demands very low cabin noise, highly tracked speed vs torque characteristics for intuitive motion control, good amount of power density and also an achievable efficiency. All these criteria fulfilled by a smooth e-drive operation with Permanent magnet synchronous BLDC motor. This kind of set-up have a challenge to overcome, that is to design best possible commutation for the three-phase inverter to achieve the speed tracking of PMBLDC motor without a significant lag. Many works have been designed and tested for an efficient control of BLDC motor [1-3]. The BLDC motor along with battery, DC/DC converter and DC/Inverter constitute the important components of EV system. In this work, attempt has been made to control the BLDC motor with only single inverter instead of combination of DC/DC converter and inverter to achieve robust performance. With the well-known topology, that is combination of DC/DC converter and inverter with a chopper, the e-drive is able to achieve the DC source average voltage as shown in Fig 1. Hence, motor received averaged effective voltage but not performing any phase switching. Here, the inverter commutating phases would be energised with a constant voltage drop with respect to corresponding sector [4-5].

This paper tries to eliminate the use of DC-DC converter and design the commutation technique while sending the PWM signal directly to inverter and activate the desired phases with respect to the motor sector positions. With the absence of one power electronics circuit, this topology will save much in terms of cost. Many works have

been reported to generate desired PWM signal to control inverter. Mainly, meta-heuristic optimisation techniques like Fuzzy, genetic algorithm, etc based PID design is used in [6-9]. Apart from meta-heuristic based PID design, some advanced control techniques like model predictive control, sliding mode control, observer based control are also used in [10-20].

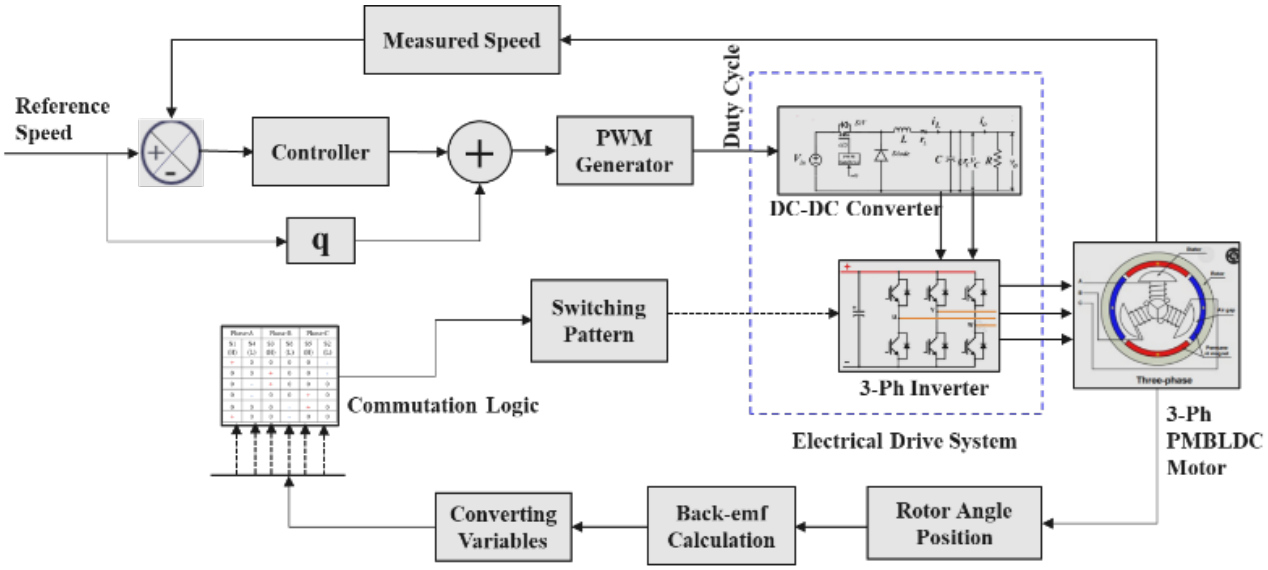

Fig. 1 *Topology with DC-DC and Inverter combination for PMBLDC motor control*

Despite having many advance control techniques, we choose to design PID control, as its already proven and easy to validate experimentally. The PID gains can be obtained through many ways e.g., ZN computing method, using metaheuristic optimization, pole placement method or iterative method [21]. Here we opt to use pole placement technique because this technique is more intuitive and handier to use when the plant model is known [22]. However, the challenge is to get surety of the dominant pole placement. In [23]-[24], a guaranteed dominant pole placement is attempted while using root locus and Nyquist criteria. In this paper, effort has been made to use pole placement technique to place the dominant poles of the system. In this paper, a dominant pole placement based PID controller design is presented for the feedback loop. Afterwards, effort made to make the system more efficient in terms of system input output loop performance through feedforward control design. A hardware setup with three-phase PMBLDC motor and kollmorgen AKD interface device developed. The results are verified with the close loop system experimentally.

The main aids of this paper are

i. E-drive setup without the modulated voltage input but able to achieve the correct set of commutation of inverter action.
ii. Achieved robust loop performance with a proportional-integral-derivative control design using pole placement method.
iii. Ensure faster input output performance while using feed forward gain design and the system is validated with an experimental hardware setup.

This paper is formatted as follows,
Section 2 represents modelling of PMBLDC motor. In section 3, the operation with proposed PID controller & pole placement technique has been discussed. In section number 4, the outcomes are shown. And in the last section 5, the conclusion has been drawn.

2. Motor Dynamic Model

The equivalent circuit diagram of a 3-Ø BLDC motor is shown in Fig. 2. The 3-Ø BLDC motor is connected through a star configuration, fed by a conventional 3-Ø VSI. The voltage equations of 3-Ø windings with phase variables are as follows:

Int. Journal of Integrated Engineering Vol. 16 No. 5 (2024) p. 250-264

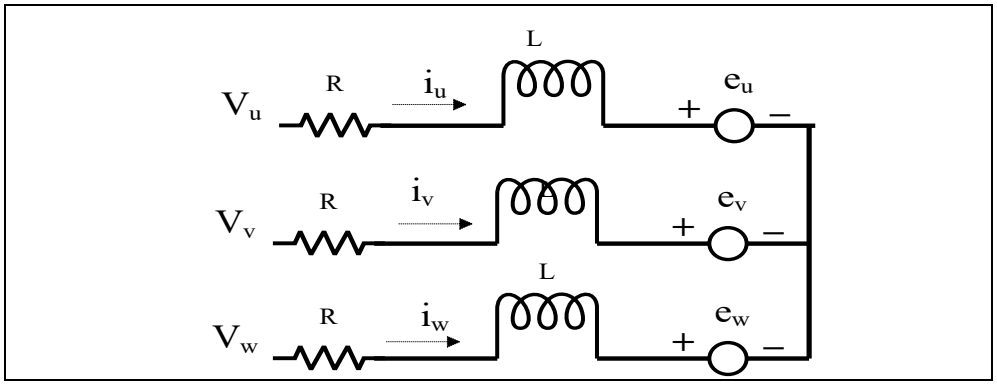

Fig. 2 *Equivalent circuit diagram of BLDC motor*

$$V_{ux} = R_r i_{ux} + L_l \frac{\partial i_{ux}}{\partial t} + M_m \frac{\partial i_{vx}}{\partial t} + M_m \frac{\partial i_{wx}}{\partial t} + e_u$$

$$V_{vx} = R_r i_{vx} + L_l \frac{\partial i_{vx}}{\partial t} + M_m \frac{\partial i_{ux}}{\partial t} + M_m \frac{\partial i_{wx}}{\partial t} + e_v$$

$$V_{wx} = R_r i_{wx} + L_l \frac{\partial i_{wx}}{\partial t} + M_m \frac{\partial i_{ux}}{\partial t} + M_m \frac{\partial i_{vx}}{\partial t} + e_w \quad (1)$$

Here, phase voltages are V_{ux}, V_{vx}, V_{wx}, and the corresponding phase currents are defined as i_{ux}, i_{vx}, i_{wx}. Back EMFs are e_u, e_v, e_w. Also, R_r is the phase resistance and L_l is the self-inductance of each individual phase. The back emfs are related as

$$\begin{vmatrix} e_u \\ e_v \\ e_w \end{vmatrix} = \omega_r \Psi_x \begin{vmatrix} f_{ux(\theta_{rad})} \\ f_{vx(\theta_{rad})} \\ f_{wx(\theta_{rad})} \end{vmatrix} \quad (2)$$

where ω_r is angular velocity. The back emf can be rewritten as

$$e_u = k\omega_r f(\theta_{rad})$$

$$e_v = k\omega_r f\left(\theta_{rad} - \frac{2\pi}{3}\right) \quad (3)$$

$$e_w = k\omega_r f\left(\theta_{rad} + \frac{2\pi}{3}\right)$$

So, star Connected three-phase current become

$$i_{ux} + i_{vx} + i_{wx} = 0 \quad (4)$$

which can also be written as

$$M_m i_{vx} + M_m i_{wx} = -M_m i_{ux} \quad (5)$$

Substituting, equation (5) in equation (1)

$$\begin{bmatrix} V_{ux} \\ V_{vx} \\ V_{wx} \end{bmatrix} = \begin{bmatrix} R_r & 0 & 0 \\ 0 & R_r & 0 \\ 0 & 0 & R_r \end{bmatrix} \begin{bmatrix} i_{ux} \\ i_{vx} \\ i_{wx} \end{bmatrix} + \begin{bmatrix} L_l - M_m & 0 & 0 \\ 0 & L_l - M_m & 0 \\ 0 & 0 & L_l - M_m \end{bmatrix} \frac{d}{dt} \begin{bmatrix} i_{ux} \\ i_{vx} \\ i_{wx} \end{bmatrix} + \begin{bmatrix} e_u \\ e_v \\ e_w \end{bmatrix} \quad (6)$$

The torque equation can be expressed as

$$J_m \frac{\partial \omega_r}{\partial t} + B_m \omega_r = T_{qm} - T_{qload} \tag{7}$$

Further, the torque developed in the motor can be written as

$$\frac{\partial \omega_r}{\partial t} = \frac{1}{J_m}\left(T_{qm} - T_{qload}\right) - B_m \omega_r \tag{8}$$

where J_m, and B_m, are the moment of inertia and frictional coefficient, respectively. Combining (6) and (7), the state-space model of the BLDC becomes

$$\dot{X} = Ax + Bu, Y = Cx \tag{9}$$

Where, $\dot{X} = [i_{ux}\ i_{vx}\ i_{wx}\ \omega_r\ \theta_{rad}]^T$, $Y = [i_{ux}\ i_{vx}\ i_{wx}\ \omega_r\ \theta_{rad}]^T$ and $u = [V_{ux}\ V_{vx}\ V_{wx}\ T_{load}]^T$

$$A = \begin{bmatrix} -\frac{R_r}{L_l - M_m} & 0 & 0 & \frac{-\psi_x}{L_l - M_m} f_{ux}(\theta_{rad}) & 0 \\ 0 & -\frac{R_r}{L_l - M_m} & 0 & \frac{-\psi_x}{L_l - M_m} f_{vx}(\theta_{rad}) & 0 \\ 0 & 0 & -\frac{R_r}{L_l - M_m} & \frac{-\psi_x}{L_l - M_m} f_{wx}(\theta_{rad}) & 0 \\ \frac{\psi_x}{J_m} f_{ux}(\theta_{rad}) & \frac{\psi_x}{J_m} f_{vx}(\theta_{rad}) & \frac{\psi_x}{J_m} f_{wx}(\theta_{rad}) & -\frac{B}{J_m} & 0 \\ 0 & 0 & 0 & \frac{P}{2} & 0 \end{bmatrix} \tag{10}$$

$$B = \begin{bmatrix} \frac{1}{L_l - M_m} & 0 & 0 & 0 \\ 0 & \frac{1}{L_l - M_m} & 0 & 0 \\ 0 & 0 & \frac{1}{L_l - M_m} & 0 \\ 0 & 0 & 0 & -\frac{1}{J_m} \end{bmatrix}, \quad C = \begin{bmatrix} 1 & 0 & 0 & 0 \\ 0 & 1 & 0 & 0 \\ -1 & 1 & 0 & 0 \\ 0 & 0 & 1 & 0 \\ 0 & 0 & 0 & 1 \end{bmatrix}$$

$$u = [V_{ux} \quad V_{vx} \quad V_{wx} \quad T_{load}]^T, e = [e_u \quad e_v \quad e_w]^T$$

Further, the transfer function of the motor can be obtained in term of speed as

$$\frac{I(s)}{V(s) - V_B(s)} = \frac{1}{sL_l + R_r} \tag{11}$$

$$\frac{\omega_r(s)}{T_{qload}(s) - T_{qm}(s)} = \frac{1}{sJ_m - B_m} \tag{12}$$

As the value of k_m and k_b are same (refer table 1), one can write

$$\frac{\omega_r(s)}{V(s)} = \frac{k_m}{(sL_l + R_r)\,(sJ_m + B_m) + k_m^2} \tag{13}$$

Int. Journal of Integrated Engineering Vol. 16 No. 5 (2024) p. 250-264

3. Proposed Control Schemes

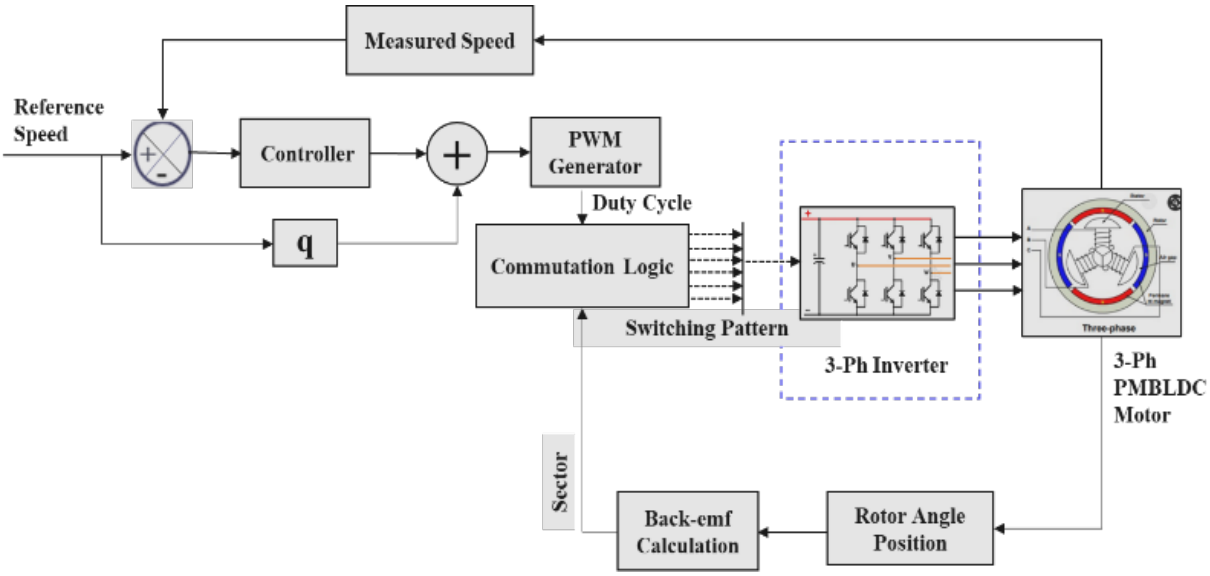

Fig. 3 *Proposed topology of inverter control PMBLDC motor without DC-DC converter*

The proposed control topology is shown in Fig. 3. The topology consists of mainly three design parts, (i) Identification of motor rotor position and selection of sector (ii) Feedback loop design, and (iii) Feedforward loop design.

3.1 Identification of The Motor Position and Selection of Sector

Throughout the operation, only two phases of BLDC motor are conducting at a given individual time slot. The sector wise inverter commutation operation is shown in Fig. 4. Here, direct back EMF zero crossing technique (Terminal Voltage Detection with Trapezoidal Control) is used to identify the sectors. As shown in Fig. 4 during zero-crossing event, the non-conducting phase back emf crosses zero as well (aligned with dashed line in Fig. 4).

Figure 4 demonstrates the concept of the 300 electrical degrees delay from the zero-crossing event. Here any speed variations don't have any impact on the delay. So, the non-conducting phase back emf is under monitor to detect the zero-crossing point. From Fig. 4, the proposed control switching logic is investigated and presented in Table 1 and Table 2. During each PWM period, the commutating phases switched in between $\pm$ 300V in a harmonizing way. At a time, one phase is connected with +ve voltage, and other is connected with -ve voltage (refer Table -1). Hence, this implement a reverse switching pattern and used the same with coupled PWM signal (refer Table -2). Here, PWM switching threshold is set to 50% of the magnitude. Therefore, based on PWM width, the sector will perform the corresponding switching pattern. The operational logic of the above two tables is presented in Fig. 5.

3.2 Linear Controller (PID) Design and Tuning

The closed-loop system containing the feedback and feedforward loop is shown in Fig. 3. The feedback loop consists of PID control and feedforward loop contain a static gain q.

3.2.1 Design of The Feedback Loop

Here, decentralized approach is used to design PID controller for the feedback loop of the MIMO system. Here the PID controller is designed for the diagonal component of the MIMO system. The controller is designed to be robust enough to counter the effect of the off-diagonal component of the MIMO system. To accomplish the motor speed tracking and control of the same, the inverter switching is modulated with the varying inputs from the PID controller, which defines the range of PWM signals for inverter commutation control.

Here the plant is

$$G(s) = \frac{N(s)}{D(s)} e^{-sL} \tag{14}$$

PID controller becomes

$$C(s) = k_p + \frac{k_i}{s} + sk_d \tag{15}$$

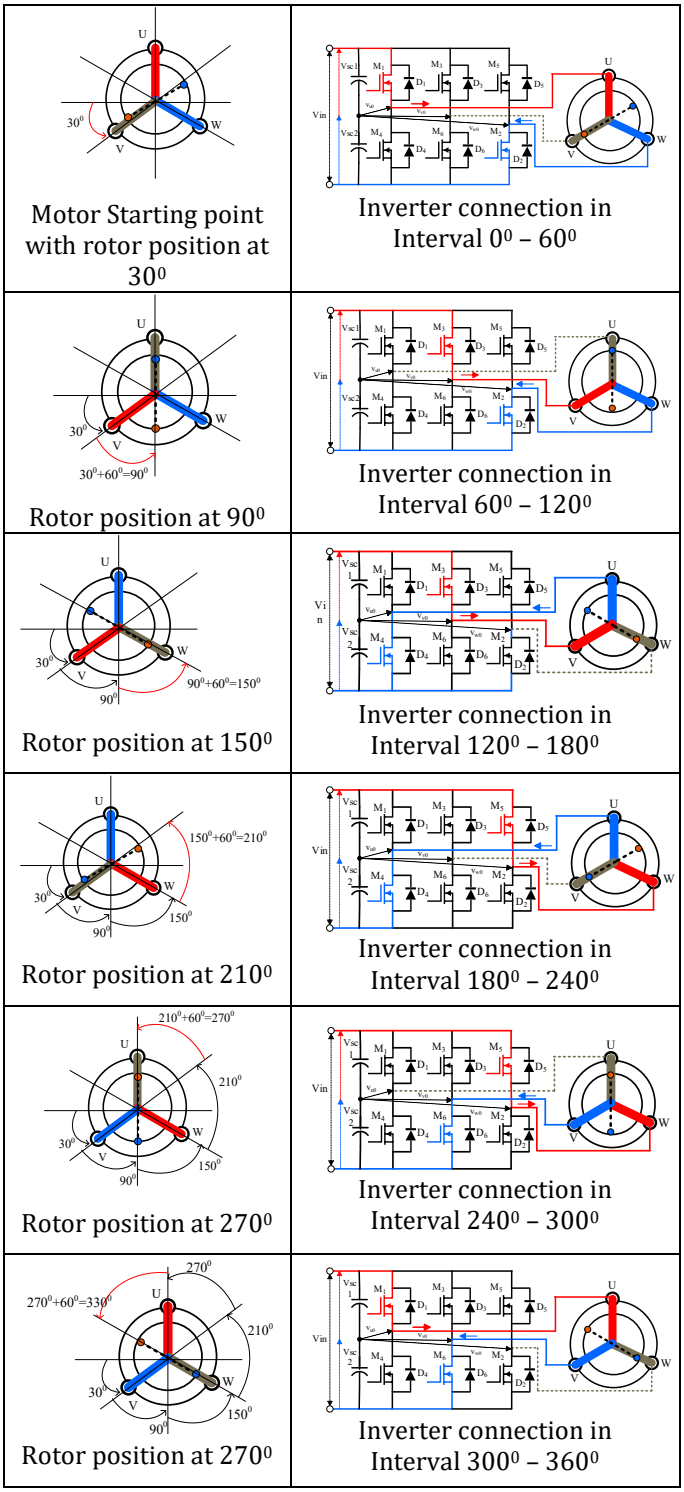

Fig. 4 *Topology of Inverter control for PMBLDC motor*

Int. Journal of Integrated Engineering Vol. 16 No. 5 (2024) p. 250-264

Now, the characteristics equation

$$1 + C(s)G(s) = 0 \tag{16}$$

Here, the placing the desired poles $\rho = -a + bj$, such a way, it will satisfy the dominant pole placement, i.e., $s = -ma$, where close loop poles should be lie in the region of m.

Hence, the characteristics equation becomes

$$k_p - \frac{k_i}{a-bj} - k_d(a - bj) = \frac{-1}{G(\rho)} \tag{17}$$

Separating the real and imaginary part, equation (17) becomes,

$$\begin{aligned} -bk_i + b(a^2 + b^2)k_d &= (a^2 + b^2)Im[\frac{-1}{G(\rho)}] \\ (a^2 + b^2)k_p - ak_i - a(a^2 + b^2)k_d &= (a^2 + b^2)Re[\frac{-1}{G(\rho)}] \end{aligned} \tag{18}$$

Since, in root locus technique, the gain is varied. Therefore, here k_p is varied to obtain the PID gains from the root locus technique. By employing the above idea, (18) can be written as

$$k_d = \frac{1}{a^2 + b^2}k_p + x^2 \tag{19}$$

$$k_i = \left[\frac{a^2 + b^2}{a} - 1\right]k_p - (a^2 + b^2)x_1 \tag{20}$$

Here, $X_2 = \frac{1}{b}\mathrm{Im}[\frac{-1}{G(\rho)}]$, and $X_1 = \frac{1}{a}\mathrm{Re}\left[\frac{-1}{G(\rho)}\right] - X_2$, by substituting the PID gains into eqn (16),

$$1 + k_p[\frac{as^2 + a(a^2 + b^2)s + (a^2 + b^2 - a)}{a(a^2 + b^2)X_2e^{-Ls}s^2 + a(a^2 + b^2)Ds - a(a^2 + b^2)X_1Ne^{-Ls}}Ne^{-Ls}] = 0$$

$$1 + k_p\bar{G}(s) = 0 \tag{21}$$

The root locus technique can be used for (21) by varying gain k_p. The design steps are outlined below

i. Draw the root locus of (21) by varying k_p.

ii. Locate the dominant pole region by choosing m.

iii. Select the interval of k_p from root locus as done in [23]-[24].

iv. From k_p, find k_i and k_d. By utilizing the above approach, the PID gains are obtained as k_p = 1.2, k_i = 0.09, and k_d = 0.05

Table 1 *Inverter switching sequence when PWM amplitude is more than 0.5*

Phase-U		Phase-V		Phase-W		Interval (Degree)
M1 (H)	M4 (L)	M3 (H)	M6 (L)	M5 (H)	M2 (L)	
+	0	0	0	0	-	0 – 60
0	0	+	0	0	-	60 – 120
0	-	+	0	0	0	120 – 180
0	-	0	0	+	0	180 – 240
0	0	0	-	+	0	240 – 300
+	0	0	-	0	0	300 – 360

Table 2 *Inverter switching sequence when PWM amplitude is less than 0.5*

Phase-U		Phase-V		Phase-W		Interval (Degree)
M1 (H)	M4 (L)	M3 (H)	M6 (L)	M5 (H)	M2 (L)	
0	-	0	0	+	0	0 – 60
0	0	0	-	+	0	60 – 120
+	0	0	-	0	0	120 – 180
+	0	0	0	0	-	180 – 240
0	0	-	0	0	+	240 – 300
0	-	+	0	0	0	300 – 360

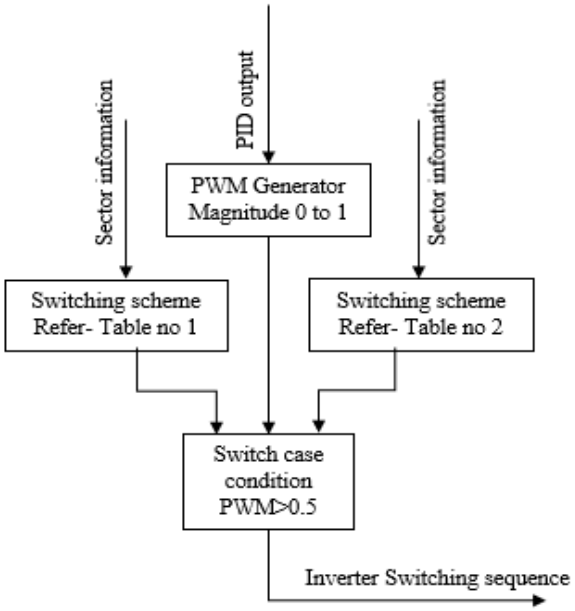

Fig. 5 *Proposed switching logic of 3-Ø inverter*

3.2.2 Feedforward Gain Design

Here, a gain q is added to obtain two-degree freedom to ensure faster input-output response. By changing the value of q, a zero location is added which makes the system faster. Here, gain q is selected iteratively so as to achieve faster input-output response. For the simulation q is chosen as 0.05. With the designed PID controller, the frequency response using the Bode plot of the system is shown in Fig. 6. Bode plot ensures enough margin (gain and phase) by the proposed method.

Int. Journal of Integrated Engineering Vol. 16 No. 5 (2024) p. 250-264

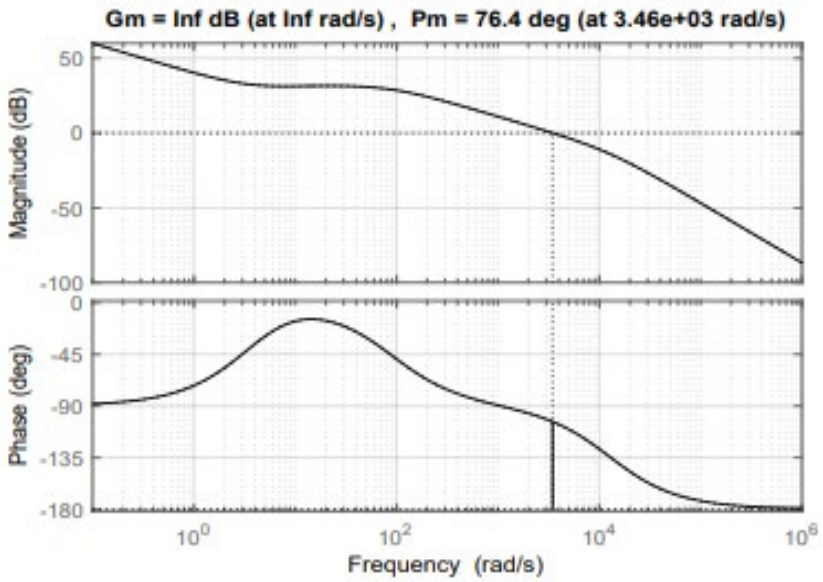

Fig. 6 *The Bode plot of the closed-loop system*

4. Experimental Results

Figure 7 shows the experimental hardware setup which is used to validate the proposed system. In Fig. 7, the PMBLDC is connected and communicated to personal computer through koll-morgen AKD interface motor drive. The designed controller is programmed and flashed in the AKD drive. The parameters used for the system is shown in Table 3.

Table 3 *Component parameters details*

Component	Used values
PMBLDC motor	Motor Speed: 0 - 3500 rpm Motor resistance (Rr): 1.292 Ω Motor inductance (Ll): 0.0001 H Motor torque constant (km): 0.0502 N.m/A Back emf constant (kb): 0.0502 V/(rad/s) Motor moment of inertia (Jm): 2.21×10−5 N.m/(rad/s2) Motor frictional coefficient (Bm): 1×10−5 N.m/(rad/s)
Battery (Lithium-ion)	Nominal voltage = 500 V Rated Capacity = 6.6 Ah
Inverter	MOSFET Drain-source on resistance, R_DS(on): 0.01 Ohm Off-state conductance: 1e-6 1/Ohm Threshold voltage : 0.5 V Integral Diode Forward voltage: 0.1 V On resistance: 0.001 Ohm Off conductance: 1e-5 1/Ohm

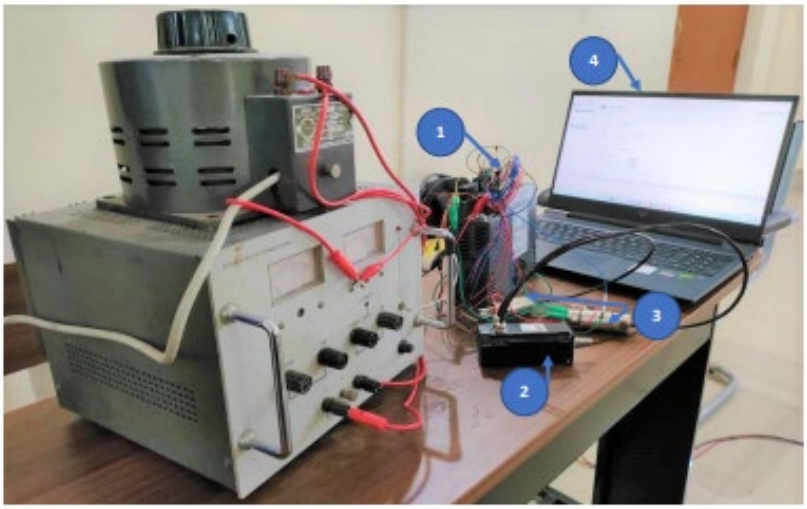

Fig. 7 *Experimental setup (1) AKD interface motor drive; (2) BLDC motor; (3) Motor terminal and encoder; and (4) Laptop*

4.1 Results of The Proposed Topology

Figure 8 shows the tracking response of the BLDC motor. To mimic the actual behaviour of electric vehicle on the track, the experiment is run for frequent acceleration and retardation. The model is run for 100 sec with acceleration, retardation and constant cruise control to verify the effectiveness of the proposed controller. From Fig. 8, it is clear that the BLDC motor is accurately tracking the set speed. Due to feed forward term, the speed of the motor is able to catch the set speed without any lag. It may also be noted that, the tracking error seems to be zero in Figure 8. However, it is usual practice to keep the error in the specified tolerance band by using integral action of PID controller. Moreover, the Fig. 8 is zoomed and the tracking response is also shown in Fig. 8 for better visibility. It may be noted that, the tracking error is well within the tolerance band.

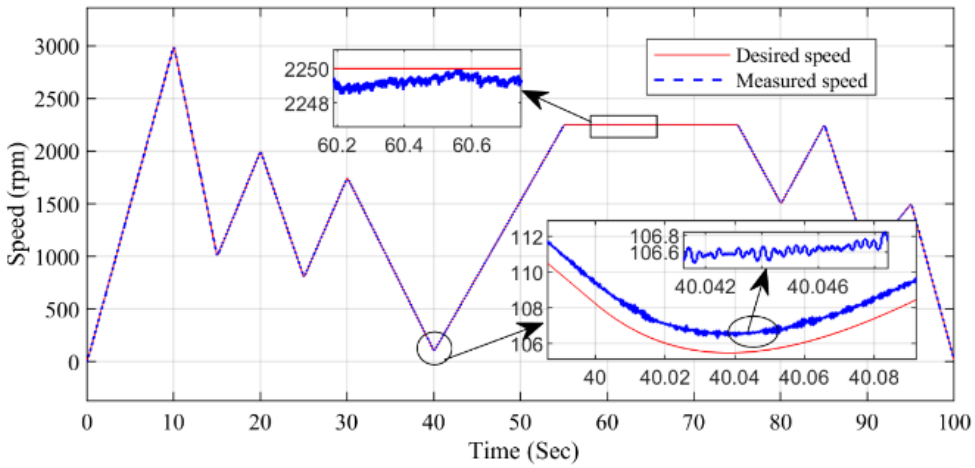

Fig. 8 *Speed tracking response of BLDC motor*

Figure 9 shows the corresponding line voltage, and different sector position during the run for 100 sec. It may be noted that the position of rotor is divided into six sectors and each sector constitutes 600 which is also zoomed and shown in Fig.9. Here, the phase voltages switches according to required motor speed by proper inverter commutation control, which is carried out by continuously sensing the sector position (defined in Fig.4). For example, when the rotor position is at sector 1 marked as circle in Fig.9, phase voltage U will be high (red colour in Fig.9) and phase voltage W will be low (blue colour in Fig.9) following Table 1. Here PWM generators switches in between two phases. These two phase voltages continue to on & off between +ve and -ve values, but stayed inside the source voltage range.

Int. Journal of Integrated Engineering Vol. 16 No. 5 (2024) p. 250-264

Figure 10 shows the output of the proposed controller and the switching signal for inverter. The controller output acts as the reference signal to PWM block and thereby the PWM generator generates the switching pulses. As shown in Fig. 10, the PWM signal magnitude varies in-between 0 to 1. Based on the PWM magnitude in each derivative, the switching sequence has been picked up by the proposed algorithm, refer Table 1 and Table 2. Further, the corresponding switching of each inverter for 120^0 mode is shown in Figure 11. Figure 11 shows the zoomed version of the commutations of the inverter switches which took place for 120^0 mode.

Figures 12 and 13 show the PMBLDC motor inputs current and voltage profile from all the three voltages and currents. As expected, the inverter having the trapezoidal current profile with the proposed control mechanism.

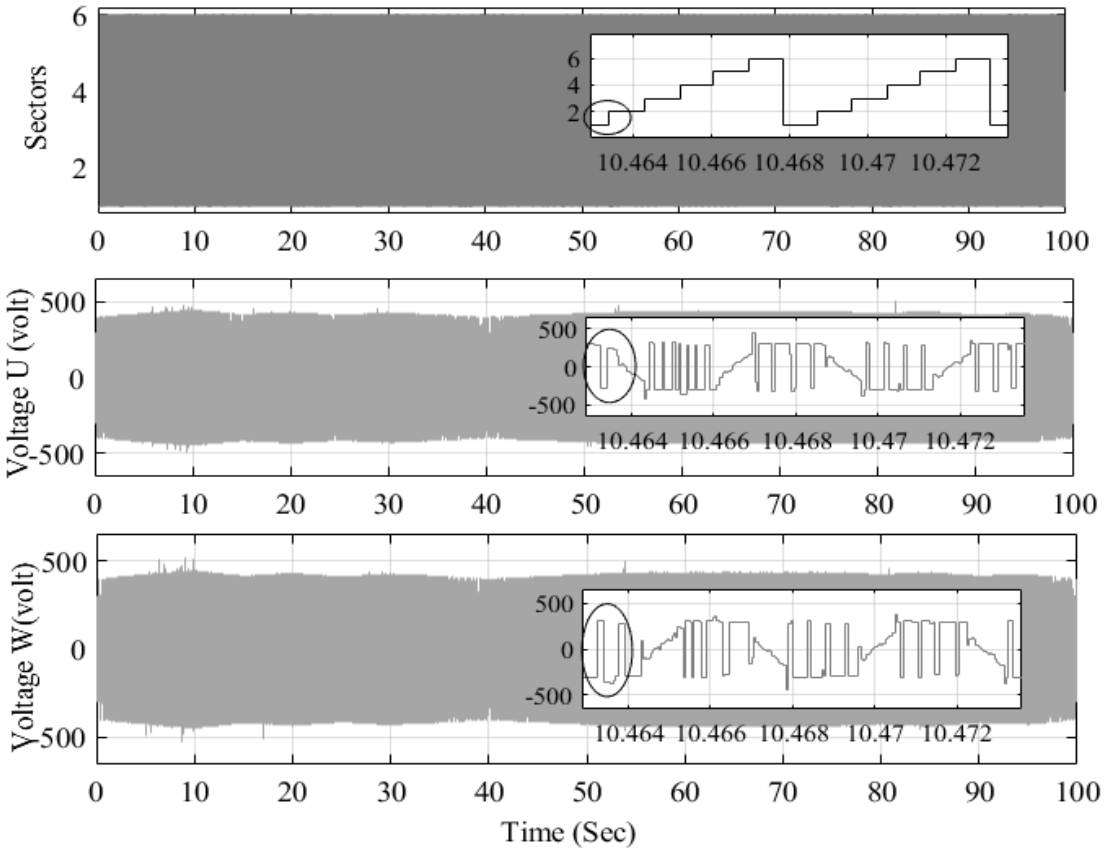

Fig. 9 *Phase voltages mapped with motor sector*

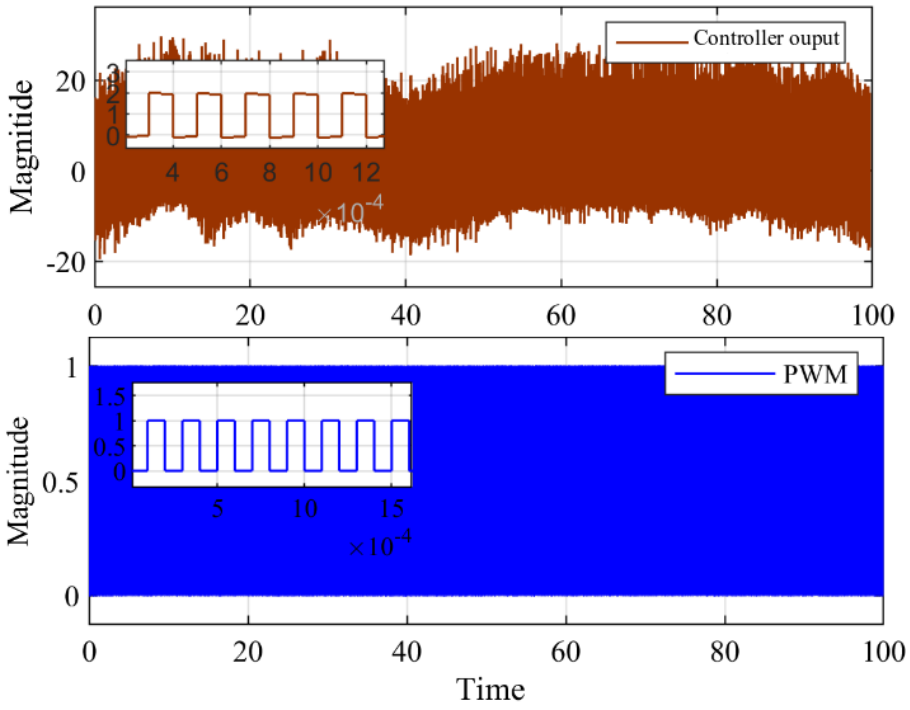

Fig. 10 *Controller output and switching signal*

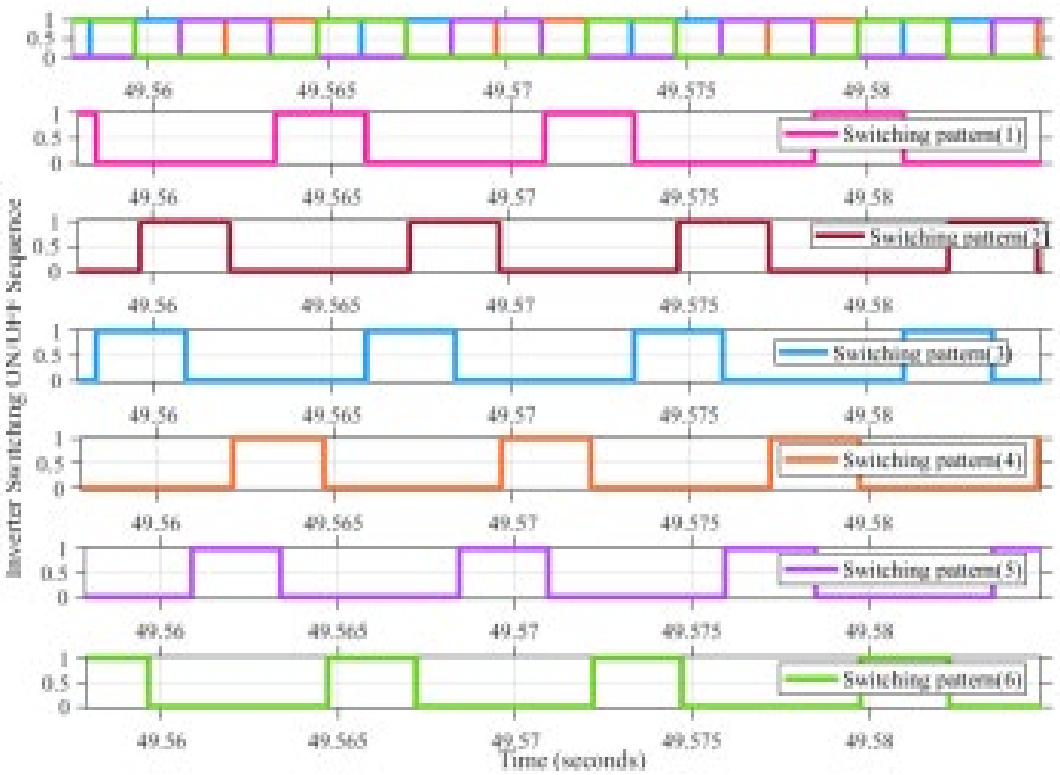

Fig. 11 *Switching signal of each inverter for 1200 mode of commutation (scaled view)*

Int. Journal of Integrated Engineering Vol. 16 No. 5 (2024) p. 250-264

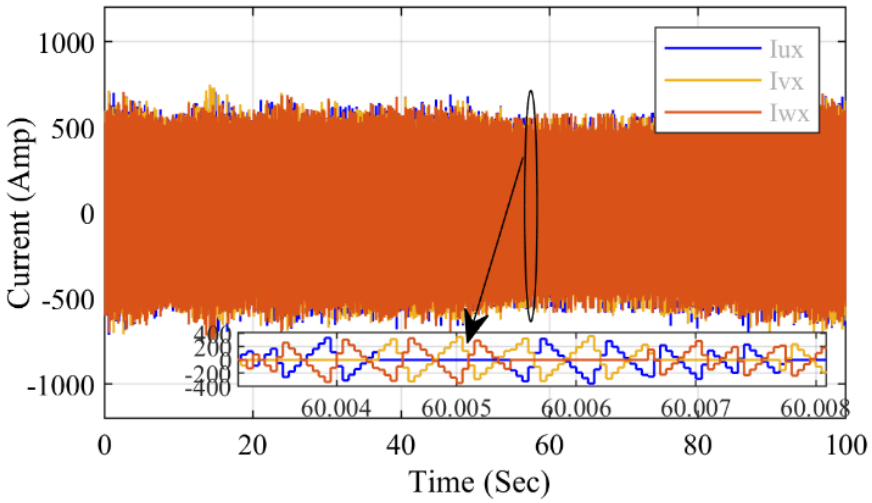

Fig. 12 *Three-phase inverter current output*

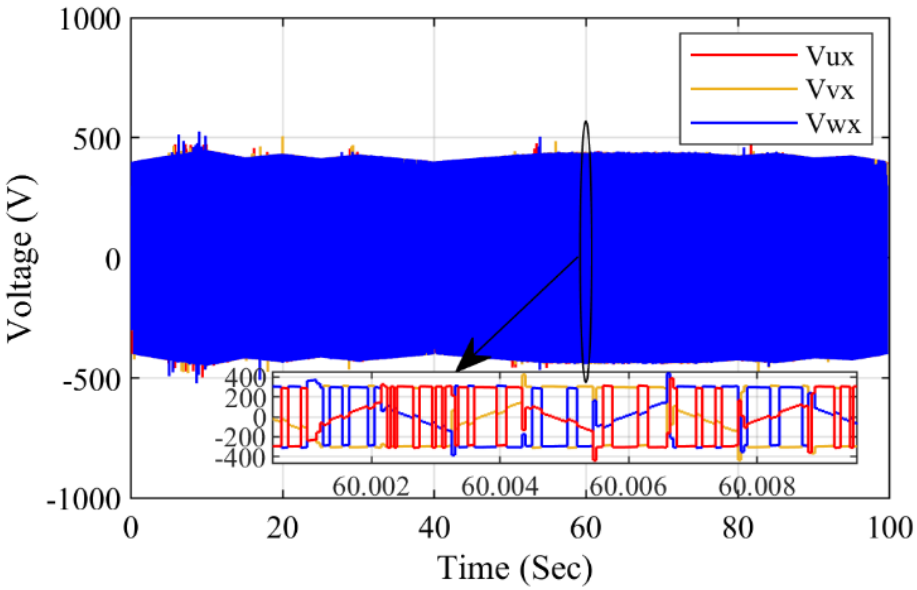

Fig. 13 *Three-phase inverter voltage output*

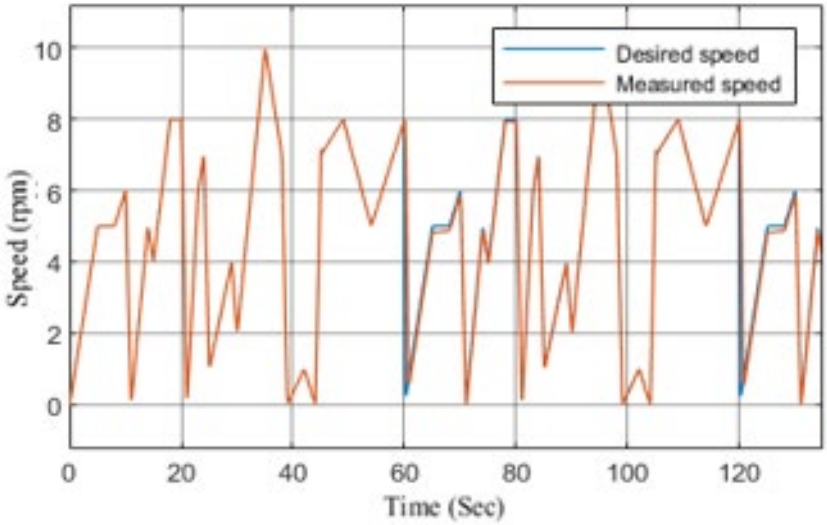

Fig. 14 *Robustness response of speed tracking*

Figure 14 demonstrates the robustness performance of the system. Here the speed demands changes abruptly with a very short time frame with less rpm. Even though this variation, the proposed system is able to achieve its performance as shown in Fig. 14. It lags to catch some very sharp rise load profile but again manage to track it without any delay.

5. Conclusions

This paper proposed an e-drive topology consisting of only one 3-phase inverter set-up to control PMBLDC motor and the performances are verified through experimentally. Unlike a dc-dc converter-based e-drive system, the proposed topology able to switch the 3-phase inverter phases correctly with PWM control technique. The inverter switching, and the two-degree-of-freedom controllers are implemented while using feedforward and feedback controllers. The feedforward controller has been tuned iteratively and the feedback controller is developed by a pole-placement approach. A PWM magnitude-based logic approach has been implemented for inverter commutation. The efficacy of the proposed topology and designed control method has been verified with a hardware experimental setup by analysing its nominal and robustness response. The e-drive performances are found satisfactory with this control method.

Acknowledgement

We thanks the anonymous reviewers for reviewing our manuscript.

Conflict of Interest

Authors declare that there is no conflict of interests regarding the publication of the paper.

Author Contribution

The authors confirm contribution to the paper as follows: ***study conception and design****: Ranjan Pramanik, Jatin K.Pradhan, B.B.Pati;* ***analysis and interpretation of results****: Ranjan Pramanik;* ***draft manuscript preparation****: Ranjan Pramanik, Jatin K.Pradhan, B.B.Pati. All authors reviewed the results and approved the final version of the manuscript.*

References

[1] Sebastiangordon, T., & Slemon, G. R. (1987). Operating limits of inverter-driven permanent magnet motor drives. *IEEE Transactions on Industry Applications*, (2), 327-333.

[2] Hong-xing, W., Shu-Kang, C., & Shu-mei, C. (2004, May). A controller of brushless DC motor for electric vehicle. In *2004 12th Symposium on Electromagnetic Launch Technology* (pp. 528-533). IEEE.

[3] Dal, Y. O. (2002, October). Influence of PWM Switching Schemes and Commutation Methods for DC and Brushless Motor Drives. In *PE Technology Conference* (pp. 27-31).

[4] Yang, H., Zhang, Y., Yuan, G., Walker, P. D., & Zhang, N. (2017). Hybrid synchronized PWM schemes for closed-loop current control of high-power motor drives. *IEEE Transactions on Industrial Electronics*, *64*(9), 6920-6929.
[5] Ramu, K. (2015). *U.S. Patent No. 8,981,705*. Washington, DC: U.S. Patent and Trademark Office.
[6] Zhu, Z. Q., Shen, J. X., & Howe, D. (2006, August). Flux-weakening characteristics of trapezoidal back-emf machines in brushless DC and AC modes. In *2006 CES/IEEE 5th International Power Electronics and Motion Control Conference* (Vol. 2, pp. 1-5). IEEE.
[7] Yang, L., Zhu, Z. Q., Gong, L., & Bin, H. (2021). PWM switching delay correction method for high-speed brushless DC drives. *IEEE Access*, *9*, 81717-81727.
[8] Lawler, J. S., Bailey, J. M., McKeever, J. W., & Pinto, J. (2002, April). Limitations of the conventional phase advance method for constant power operation of the brushless DC motor. In *Proceedings IEEE SoutheastCon 2002 (Cat. No. 02CH37283)* (pp. 174-180). IEEE.
[9] Rathore, A. K., Holtz, J., & Boller, T. (2012). Generalized optimal pulsewidth modulation of multilevel inverters for low-switching-frequency control of medium-voltage high-power industrial AC drives. *IEEE Transactions on Industrial Electronics*, *60*(10), 4215-4224.
[10] Cui, C., Liu, G., & Wang, K. (2014). A novel drive method for high-speed brushless DC motor operating in a wide range. *IEEE transactions on power electronics*, *30*(9), 4998-5008.
[11] Rong, L., Weiguo, L., & Xiangyang, L. (2007, November). A novel pm bldc motors inverter topology for extending constant power region. In *IECON 2007-33rd Annual Conference of the IEEE Industrial Electronics Society* (pp. 1233-1237). IEEE.
[12] Lawler, J. S., Bailey, J. M., McKeever, J. W., & Pinto, J. (2004). Extending the constant power speed range of the brushless DC motor through dual-mode inverter control. *IEEE transactions on power electronics*, *19*(3), 783-793.
[13] Celanovic, N., & Boroyevich, D. (2000). A comprehensive study of neutral-point voltage balancing problem in three-level neutral-point-clamped voltage source PWM inverters. *IEEE Transactions on power electronics*, *15*(2), 242-249.
[14] Lee, H. J., Kim, S., & Yoon, Y. D. (2019, September). Accurate neutral current control for neutral point voltage balancing in three-level inverters considering digital control and PWM delay. In *2019 IEEE Energy Conversion Congress and Exposition (ECCE)* (pp. 4795-4800). IEEE.
[15] Singh, A. K., & Kumar, K. (2002). Modelling and simulation of PID controller type PMBLDC motor. In *Proceedings f National Seminar on Infrastructure Development Retrospect and prospects* (Vol. 1, pp. 137-146).
[16] Ansari, U., & Alam, S. (2011, March). Modeling and control of three phase BLDC motor using PID with genetic algorithm. In *2011 UkSim 13th international conference on computer modelling and simulation* (pp. 189-194). IEEE.
[17] Chen, J., Guo, Y., & Zhu, J. (2007). Development of a high-speed permanent-magnet brushless DC motor for driving embroidery machines. *IEEE Transactions on Magnetics*, *43*(11), 4004-4009.
[18] Mohanraj, D., Aruldavid, R., Verma, R., Sathiyasekar, K., Barnawi, A. B., Chokkalingam, B., & Mihet-Popa, L. (2022). A review of BLDC motor: state of art, advanced control techniques, and applications. *Ieee Access*, *10*, 54833-54869.
[19] Kim, T. H., & Ehsani, M. (2004). Sensorless control of the BLDC motors from near-zero to high speeds. *IEEE transactions on power electronics*, *19*(6), 1635-1645.
[20] Blasko, V., Kaura, V., & Niewiadomski, W. (1997, October). Sampling of discontinuous voltage and current signals in electrical drives: A system approach. In *IAS'97. Conference Record of the 1997 IEEE Industry Applications Conference Thirty-Second IAS Annual Meeting* (Vol. 1, pp. 682-689). IEEE.
[21] Skogestad, S. (2001, November). Probably the best simple PID tuning rules in the world. In *AIChE Annual Meeting, Reno, Nevada* (Vol. 77, p. 276h). Citeseer.
[22] Kim, K., & Schaefer, R.C. (2005). Tuning a PID Controller for a Digital Excitation Control System, IEEE Transactions On Industry Applications, 41(2), 485-492.
[23] Tang, W., Wang, Q. G., Ye, Z., & Zhang, Z. (2007). PID tuning for dominant poles and phase margin. *Asian Journal of Control*, *9*(4), 466-469.
[24] Srivastava, S., Misra, A., & Sarkar, A. (2019, March). Analysis & design of robust PID controller with dominant pole placement approach. In *2019 6th International Conference on Signal Processing and Integrated Networks (SPIN)* (pp. 908-914). IEEE.